The Association of Engineering and Shipbuilding Draughtsmen.

Graphical Methods for Treating Certain Beam Problems.

(3rd Revised Reprint).

W. R. NEEDHAM.

Published by The Association of Engineering and Shipbuilding Draughtsmen,
96 St. George's Square, London, S.W.1.

SESSION 1950-51.

Printed by Milne, Tannahill & Methven, Ltd. (T.U.), 12-14 Mill Street, Perth.

ADVICE TO INTENDING AUTHORS OF A.E.S.D. PAMPHLETS.

Pamphlets submitted to the National Technical Sub-Committee for consideration with a view to publication in this series should not exceed 9,000 to 10,000 words and about 20 illustrations, making a pamphlet of about 40 to 48 pages. The aim should be the presentation of the subject clearly and concisely, avoiding digressions and redundance. Manuscripts are to be written in the third person.

Drawings for illustrations should be done either on a good plain white paper or tracing cloth, deep black Indian ink being used. For ordinary purposes they should be made about one-and-a-half times the intended finished size, and it should be arranged that wherever possible these shall not be greater than a single full page of the pamphlet, as folded pages are objectionable, although, upon occasion, unavoidable. Where drawings are made larger, involving a greater reduction, the liens should be made slightly heavier and the printing rather .arger than normal, as the greater reduction tends to make the lines appear faint and the printing excessively small in the reproduction. In the case of charts or curves set out on squared paper, either all the squares should be inked in, or the chart or curve should be retraced and the requisite squares inked in. Figures should be as self-eviednt as possible. Data should be presented in graphical form. Extensive tabular matter, if unavoidable, should be made into appendices.

Authors of pamphlets are requested to adhere to the standard symbols of the British Standards Institution, where lists of such standard symbols have been issued, as in the case of the electrical and other industries, and also to the *British Standard Engineering Symbols and Abbreviations*, No. 560, published by the B.S.I. in 1934 at 5/-. Attention might also be given to mathematical notation, where alternative methods exist, to ensure the minimum trouble in setting up by the printer.

The value of the pamphlet will be enhanced by stating where further information on the subject can be obtained. This should be given in the form of footnotes or a bibliography, including the name and initials of the author, title, publisher, and year of publication. When periodicals are referred to, volume and page also should be given. References should be checked carefully.

Manuscripts, in the first instance, should be submitted to the Editor, *The Draughtsman*, 96 St. George's Square, London, S.W.1.

For Pamphlets, a grant of £20 will be made to the Author, but special consideration will be given in the case of much larger pamphlets which may involve more than the usual amount of preparation.

The Association

of

Engineering and Shipbuilding Draughtsmen.

Graphical Methods for Treating Certain Beam Problems.

(3rd Revised Reprint.)

W. R. NEEDHAM.

Published by The Association of Engineering and Shipbuilding Draughtsmen,
96 St. George's Square, London, S.W.1

SESSION 1950-51.

1/51.

GRAPHICAL METHODS FOR TREATING CERTAIN BEAM PROBLEMS.

By W. R. NEEDHAM.

A FOREWORD to beginners who read this paper may be *apropos*. It will probably help them in understanding matters if, as they read, they carry out the instructions step by step. Then they will find an adjustable square or clinograph invaluable while executing the necessary instructions.

It is scarcely necessary to state that the writer cannot, even if he had the ability, hope in the space available to treat so big a subject at all exhaustively. The utmost he can do is to take a few fairly representative cases. It is at best rather a scrap-book method, but it should at least suggest the way to tackle many of the problems one is likely to meet.

The present edition retains extensions and modifications (including minor corrections) of the last so that any member possessing that edition needs no other.

---

1. The first case considered is that of the bending moment and reaction loads of a beam, freely supported at each end, and subjected to unequally spaced, constant, concentrated, and dissimilar loading, fixed lengthwise between supports. We shall treat the problem for three such loads.

To start then, draw to a convenient scale, h* inches per inch, the beam length, marking the relative positions of supports and loads as shown in Fig. 1. AB and EA are supports, BC, CD, and DE, the three loads. The systems being in equilibrium, the downward forces exerted by the three loads upon the beam are exactly balanced by the upward thrusts the beam receives from the two supports. This is indicated in the figure by the sensing of the various arrows shown.

Now to the right of Fig. 1 drop a vertical from a point B as per Fig. 2. This line we divide into three lengths proportional to the three beam loads, and the scale we adopt is d lbs. per inch. Thus B to C, C to D, and D to E of Fig. 2 are proportional respectively to BC, CD, and DE of Fig. 1.

* This means, of course, that the *actual* beam length is h times the length *as drawn*.

Next choose any pole OP (call it H) normal to vertical BE, intersecting it say about midway between the extremities. OP is shown dotted to avoid confusion with the other radiating lines of the figure. Join points B, C, D, and E to O. We can make the polar length anything we like, but to simplify the subsequent calculations, where English measurements are adopted, 10 inches is usually an ideal dimension to take. We choose 5 inches in the numerical example to follow. Throughout the paper the English system of measurements is used. At the same time, if it is not as it were introducing politics into the pulpit, it is perhaps permissible to state that there are marked advantages in the use of such a simple, logical, and uniform basis of weights and measures as the metric system undoubtedly provides. But to resume, the completed figure is a ray polygon, pointing towards Fig. 1, which is the preferable construction.

Now drop an ordinate from each support and load centre of Fig. 1, as shown to chain dotted lines, through Fig. 3. Specially observe the notation used. It is probably due to Bow, and has also been adopted by Goodman. Starting outside the right-hand support AB, we mark that space A, the space between support and the first load is B, between first and second loads C, second and third loads D, third load and left-hand support E, and outside that support A again. We consider these two spaces A as one continuous stretch reaching outwards from each support, then bending backwards and meeting behind the figure. Now label the supports and loads thus :—right-hand support between spaces A and B is AB, similarly first load is BC, second CD, third DE, and left-hand support EA.

Next, in space B draw a line parallel to BO of ray polygon. Similarly the link stretching across space C of Fig. 3 is parallel to CO of Fig. 2. This line joins the first link at the downward projection of BC, and is itself continued by the third link spanning space D, which in turn is parallel to DO of ray figure. The last link across space E is parallel to EO of Fig. 2. We now close the figure by joining the extremities, as shown by chain dotted line. This completes the link polygon Fig. 3. Now from polar point O, in Fig. 2, draw OA parallel to resultant line just described. Where OA—also shown chain dotted—intersects BE in A, the point A divides the vertical into lengths proportional to the reactions AB and EA. Thus distance A to B into scale d = magnitude of reaction load AB (Fig. 1), and E to A into d = reaction load EA, *e.g.*, if we assume A to B measures 1·5 in., and d = 200 lbs. per inch, then reaction AB = $1{\cdot}5 \times 200 = 300$ lbs. Now observe the notation in the load line of Fig. 2. A to B is upwards ; B to C, C to D, and D to E are downwards ; while E to A is upwards again. All this agrees with direction of arrows shown in Fig. 1, the loads

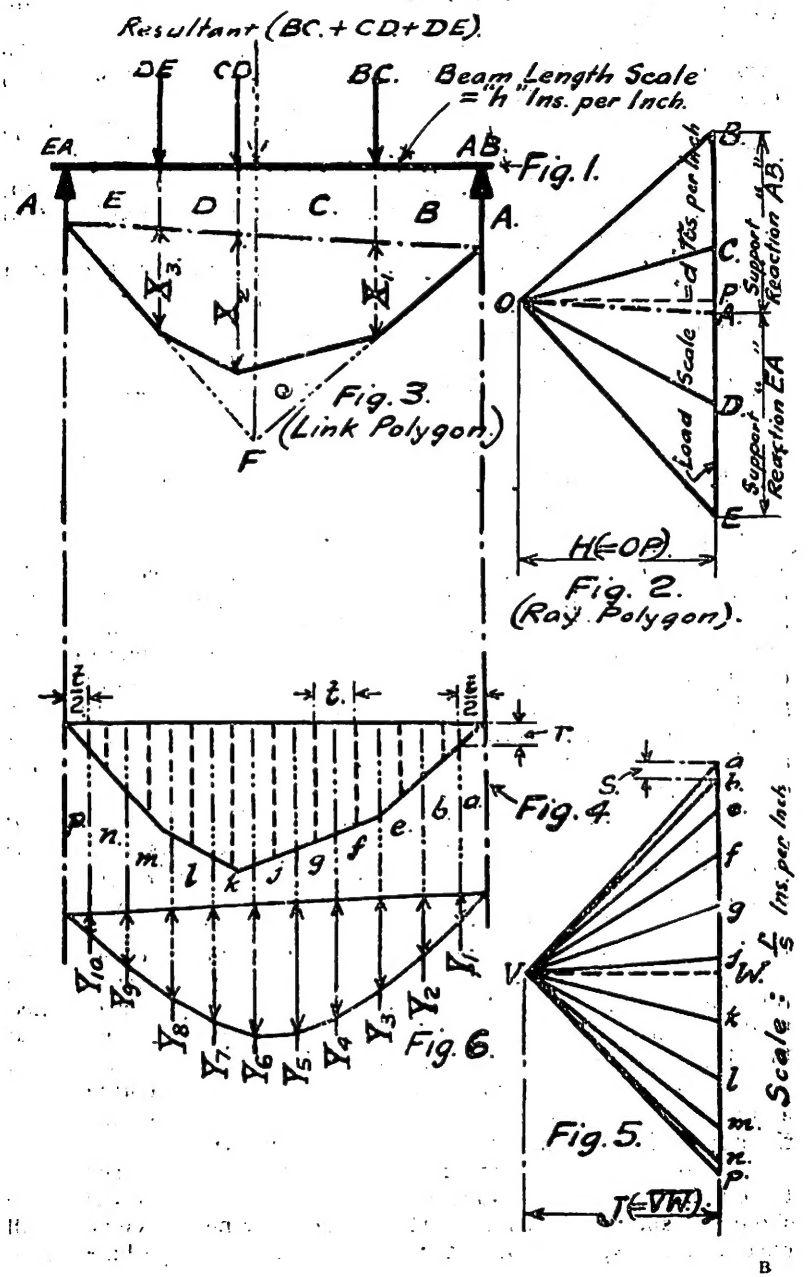
Resultant (BC.+CD+DE).
DE
CD
BC.
Beam Length Scale = "h" Ins. per Inch.
EA.
AB.
Fig. 1.
A.
E
D
C.
B
A.
Fig. 3.
(Link Polygon)
F
O
B.
C.
D.
E
Load Scale "d" Lbs. per Inch
Support Reaction AB.
Support Reaction EA
H(=OP).
Fig. 2.
(Ray Polygon).
Unit
Unit
t.
T.
Fig. 4.
S.
a
b
c
d
e
f
g
h
k
l
m
n
p
V
W.
Scale: T/S Lbs. per Inch
J(=VW).
Fig. 5.
Fig. 6.

acting downwards upon the beam, while the supports thrust upwards against it.

It may be of interest to notice that if we continue inwards the two-end links of Fig. 3 till they meet in F, the vertical projection of F upwards on to the beam marks the lengthwise position of the resultant of loads BC, CD, and DE. The centre of gravity of the system coincides with this position.

Now the link polygon, Fig. 3, is the bending moment diagram, and the bending moment at any axial position is proportional to the depth of the diagram at that position.

These various depths are marked X_1, X_2, X_3, and the maximum bending moment is at X_2.

Now maximum Bm. (at X_2) = X_2. d. H. h. lb. inches,
where X_2 is measured in inches,

d = scale of vertical line, Fig. 2 (in lbs. per inch),
H = length of pole in inches, Fig. 2,
h = scale of beam length, Fig. 1 (in inches per inch).

Thus, if $X_2 = \cdot 8''$, $d = 200$ lbs. per inch, $H = 5''$, $h = 10''$ per inch, Bm. $= \cdot 8 \times 200 \times 5 \times 10 = 8{,}000$ lb. inches.

It is perhaps well to recall that in practice we seldom if ever get a truly concentrated as distinct from a distributed load. In other words, there is seldom if ever an application point strictly considered—it is rather an application surface. What often happens is that we have several loading units, each more or less equally distributed along its limited length. If we want really good results we divide each unit into a number of vertical sections. We then take the weight of each part, assuming it concentrated at its centre of gravity. Ordinates are dropped from gravity centres, and the process already illustrated is carried through. These refinements, however, are seldom needful, though in a few cases it may be advisable to extend the detail work, as for instance where we wish to economise in material and yet keep the deflection within prescribed limits.

It may be interesting also to remember that an equally distributed load is compounded of an infinite number of infinitely small, equal, concentrated loads, of equal but infinitely minute pitching. To sum up, then, we do not get a truly concentrated load, but a succession of distributed loads; and yet each distributed load is really an extended series of the minutest concentrated loads.

It is probably quite unnecessary to add that the bending stress at any beam section is the quotient of the bending moment over the section bending modulus (the Z_{Bm}) of that section.

The proof for the bending moment diagram is a somewhat tedious business. If we are content to take a hint, however, we should be speedily satisfied. It will probably be sufficient for all except that hypercritical attitude of mind which, perhaps justi-

fiably enough, rejects certain of Euclid's so-called axioms as axioms. We can readily imagine the late Mr. Gilbert K. Chesterton, that master of paradox, telling us that an axiom may be anything under the sun except axiomatic.

We know that the bending moment, say at X_1 of Fig. 3, is actually load AB into arm B. Now the triangle in space B of Fig. 3 is identical in form, though reversed and of different size, to the triangle AOB of Fig. 2. Then distance AB of Fig. 2 into d = load AB of Fig. 1. Also actual arm B (Fig. 1) = B. h inches.

$\therefore$ Bending moment = AB. d. B. h lb. inches (1).

If we compare the similar triangles, then $\frac{X_1}{B} = \frac{AB}{H}$;

$\therefore$ X_1. H = AB. B.

Substitute X_1. H for AB. B in (1), and bending moment = X_1. d. H. h. lb. inches.

2. We are now to treat graphically the deflection of the beam system already described, where the beam is of uniform cross section throughout. This is the simplest form of the problem.

While some may consider the foregoing little better than glorified kindergarten work, it forms the necessary basis for what is to follow. At the worst is has been repetition ; at the best shall we say a refresher and a stepping-stone ?

The bending moment diagram, Fig. 3, is the framework for our succeeding structure. Now divide this diagram into a number of vertical strips of width t (Fig. 4). For obvious reasons ten divisions are often made. Next bisect each strip width, and from the mid positions drop ordinates, as shown in Fig. 4. There are also two end ordinates, one projected from each support centre. The spaces between the ordinates are lettered here a to p. The pitches a and p each = $\frac{t}{2}$, while each one of the others = t. This done, measure the depth of the diagram, Fig. 4, at each ordinate. The first right-hand strip ordinate is shown as r. Now mark off these various depths to a suitable scale on the vertical of a second ray polygon (Fig. 5). Thus a to b (given as s) of vertical in Fig. 5 is proportional to depth r of Fig. 4, and the other depths are arranged similarly. Hence scale of vertical is $\frac{r}{s}$ inches per inch.

Next, in Fig. 5, choose any pole J = VW (shown dotted) normal to the vertical, where V is the polar point and W usually about midway between extremities of vertical. It is desirable, though not always practicable perhaps, to make this pole length J = pole length H (of Fig. 2).

We are now able, by exactly following the method described for Fig. 3, to plot the final link polygon, Fig. 6. This is the deflection diagram. Thus line spanning *a* is parallel to *a* V of ray polygon, and so with all the links, till finally *p* V of Fig. 5 is parallel to line stretching across space *p* of deflection diagram. The line joining the link extremities completes the polygon. Now the beam deflection along its length varies as the corresponding depths of this diagram. The various ordinate depths are lettered Y_1, Y_2, etc., to Y_{10}. The maximum deflection actually lies between Y_5 and Y_6. Call it Y_5. Then maximum deflection

$$= \frac{Y_5.\ t.\ d.\ \text{H.}\ \text{J.}\ h^3.\ r.}{\text{E.}\ \text{I.}\ s.}\ \text{inches},$$

where Y_5 is measured in inches,
t = strip width in inches (Fig. 4),
d. H. *h*. are as already given for Bm. diagram,
J = length of pole in inches, Fig. 5,
r = mean depth in inches of any strip in Fig. 4, and
s = corresponding proportional depth in inches on vertical of Fig. 5.
E = mod. of elasticity for material of beam, lbs. per sq. in.,
I = moment of inertia (bending) of beam section.

If we put *d*. H. *h* (already obtained for bending moment) = R,

then maximum deflection $= \dfrac{Y_5.\ t.\ \text{R.}\ h^2.\ \text{J.}\ r}{\text{E.}\ \text{I.}\ s.}$ inches.

According numerical values to symbols thus : $Y_5 = \cdot 9$, $t = \cdot 15$, R = 10,000, $h = 10$, J = 5, $r = \cdot 15$, E = 30×10^6, I = 35, $s = \cdot 075$,

then δ maximum $= \dfrac{\cdot 9 \times 1 \cdot 5 \times 10{,}000 \times 10^2 \times 5 \times \cdot 15}{30{,}000{,}000 \times 35 \times \cdot 075} = \cdot 01285$ in.

The maximum deflection of such a uniform section beam occurs never far from the centre of span, and the limit of variation either way does not exceed 8 per cent. of the span length. It may be greatly different, however, in the case of certain stepped beams.

For quick work it is not a bad plan to use squared paper. It answers well enough for ordinary purposes where extreme *finesse* is not deemed necessary. Thus, with English squares, each main one-inch division would be made to represent 5, 10, 15, 20 inches, etc., respectively, as may prove most convenient ; whence *h* would be, of course, correspondingly 5, 10, 15, 20, etc., inches per inch, as the case may be. It is obvious we reduce the drudgery, since our ordinates are already at hand. The necessary construction work can be negotiated by *moving the squared paper* as required, under the *held tee square*. If we adopt this method we need neither clinograph nor even drawing pins, but obviously great care must

be taken in manipulation. For really close results, however, the more conventional practice is far preferable.

Perhaps one other point might be mentioned in passing. In the treatment just considered, slightly closer results would be obtained if the ordinates, dropped through Fig. 6, were taken from the respective centres of gravity instead of the mid-strip widths of the sub-areas of Fig. 4. The measured depths, however, upon which the divisions in the vertical of Fig. 5 are based, are rightly taken as average depths. They remain, therefore, as already given, mid-strip depths. In other words, r and s are not at all affected by the refinement. It is a refinement in any case which seldom affects the result more than an odd percentage or so. If the sub-divisions of the bending moment diagram were extremely coarse, then the divergence might become serious.

And now just a hint explanatory to the building up of the deflection formula :—Deflection as we know $= k \frac{W. L^3}{E. I}$, where k is a constant whose value depends upon the nature of the loading and the method of support. This, however, is to state a result, not outline a development. Deflection is numerically equal to the moment of each tiny area element of the bending moment diagram about the free end (or centre of free support), over E into I. Think that out, and we find that these areas are expressed in certain WL depth into L length terms, and the arm of each such moment also in L terms. Thus we get our WL^3 factors of the formula.

Now 1-inch depth of bending moment diagram, Fig. 3 = $d.$ H. $h.$ lb. inches; so one square inch represents $d.$ H. h^2 lb. inches^2 and t square inches give $t.\ d.$ H. h^3 lb. inches^2. Then area $t.\ r$ represents $t.\ r.\ d.$ H. h^2 lb. inches^2. Since, however, r is put as s on vertical, Fig. 5, the scale is now $\frac{t.\ r.\ d.\ \text{H.}\ h^2}{s}$. Introduce here the E. I. factors not required in the graphical process, and we get Y″ depth of deflection diagram, Fig. 6, = Y. $\frac{\left(\frac{t.\ r.\ d.\ \text{H.}\ h^2}{s}\right)}{E.\ I.}$ J. h inches, and maximum deflection (at say Y_5) $= \frac{Y_5.\ t.\ r.\ d.\ \text{H.}\ J.\ h^3}{E.\ I.\ s.}$ inches.

3. The next problem is that of the deflection of a beam similarly loaded, but of variable cross section.

For the bending moment diagram we simply adopt the methods already described for Figs. 1 to 3. Figs. 7, 8 and 9 show the system

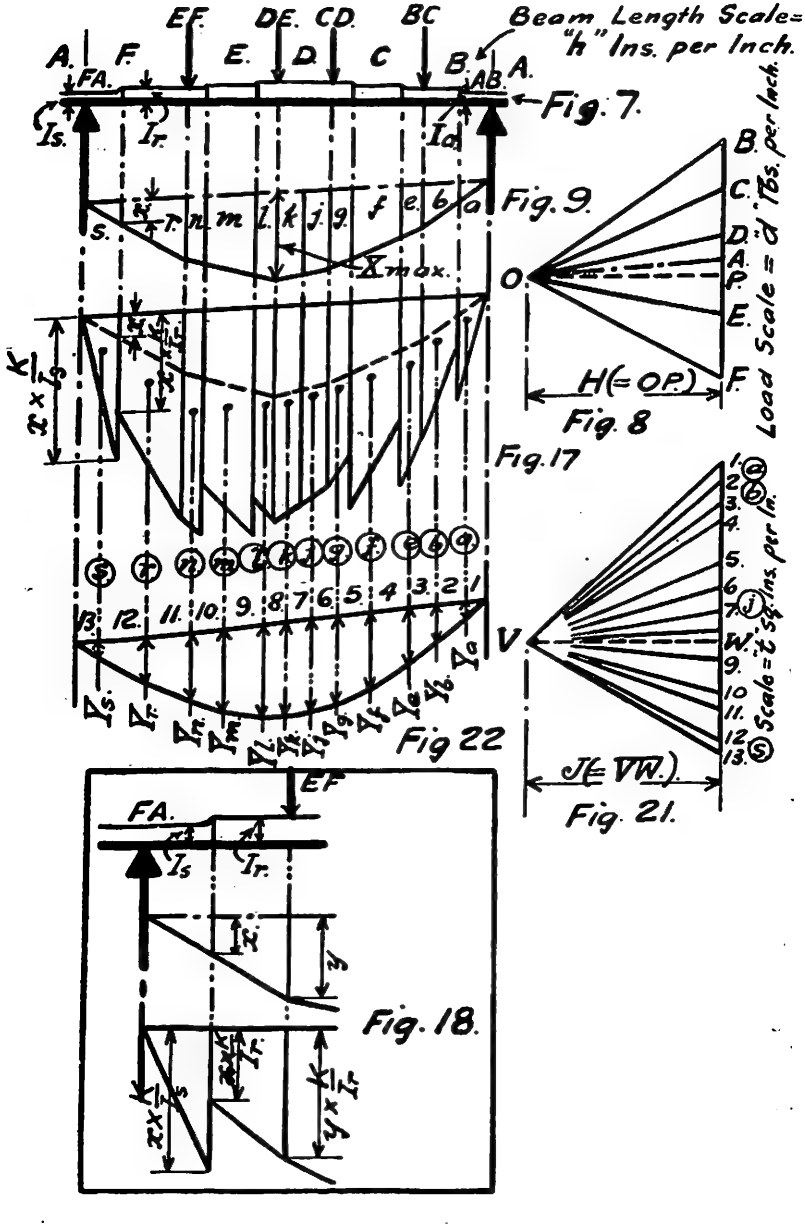
EF
DE
CD
BC
Beam Length Scale= "h" Ins. per Inch.
A.
F.
E.
D.
C
B.
A.
FA.
AB.
Fig. 7.
Is.
Ir.
Io
Fig. 9.
Xmax.
Fig. 8
H(=OP)
Load Scale = d Lbs. per Inch.
Fig. 17
Fig. 22
Scale = t Sq. Ins. per In.
JK(=VW.)
Fig. 21.
Fig. 18.

and illustrate the stages. Here, however, we have taken four concentrated loads. Fig. 7 also shows the varying section of the beam, which at the left-hand support is marked I_s, then I_r; and the last section at the right-hand support is I_a. The suffixes *s* to *a* correspond to the different space markings of the top link polygon. We sub-divide this polygon, Fig. 9, into a number of vertical sections whose boundaries are ordinates projected from beam shoulders, support and load centres, and any intermediate position deemed necessary, *e.g.*, the ordinate between *j* and *k*. These section areas, *a* to *s* inclusive, form the basis for the vertical of a second ray polygon, Fig. 21.

Each depth, however, must first be multiplied by $\frac{K}{I}$, where K is a convenient constant often not less in value than the maximum I of the beam. In this particular example, since the sub-areas *g* to *l* inclusive of Figs. 9 and 17 are concerned with the beam at its maximum I, K would be most conveniently taken as equal to that maximum I.

Notice that the extreme left-hand section of Fig. 9 is a triangle of height *x*. The product of *x* into $\frac{K}{I}$ gives us the greater depth shown in Figs. 17 and 18—which latter is added by way of amplification. It is obvious that at the apex of the triangle (regarding the vertical as its base) the product yields no change. Thus the resultant figure is also a triangle. Observe that throughout the length of section *s*, I_s is constant. At the boundary between *s* and *r*, however, I_s increases to I_r, continuing at I_r till the ordinate separating *n* from *m* is reached, where it becomes I_m. Now depth *x* being common to the triangle and its adjoining trapezium, the new depth for the right-hand figure is less than that for the triangle, since the denominator I_r is greater than I_s. And so we find each required corrected ordinate depth. Fig. 17 shows all the derived sections thus obtained throughout the whole beam length. It will be noticed that the various figures are a set of trapezia bounded by a triangle at each end. The basic bending moment diagram limits are indicated by the dotted lines. In parenthesis it may be stated (as doubtless the reader has discovered) that this expedient of multiplying throughout by $\frac{K}{I}$ is the means adopted for overcoming the complications introduced by the variability in beam cross-section. It probably provides the readiest, simplest and easiest medium for negotiating those complications.

Now, from the centre of gravity of each resultant figure, drop an ordinate. These are marked (a) to (s). We next obtain the

area of each triangle and trapezium. This done, we plot these areas to a convenient scale, say t square inches per inch, on the vertical of a ray polygon, shown completed in Fig. 21. Next, adopting our now familiar method, from Figs. 17 to 21, we are able to construct link polygon, Fig. 22, which is the deflection diagram. The various ordinate depths of the link polygon are marked Y_a to Y_s respectively, and they vary as the deflections at those positions.

$$\text{Maximum deflection (at } Y_k) = \frac{Y_k . t . d . H . J . h^3}{E . K} \text{ inches,}$$

where Y_k is measured in inches,

d = scale of vertical line (Fig. 8) in lbs. per inch,
H = length of pole in inches (Fig. 8),
J = length of pole in inches (Fig. 21),
h = beam length scale in inches per inch (Fig. 7),
t = scale of vertical line (Fig. 21) in square inches per inch,
K = convenient constant often equal to the maximum I of beam,
E = modulus of elasticity for material of beam, in lbs. per sq. inch.

For steel beams, $E = 30 \times 10^6$. Hence in such cases

$$\text{Maximum deflection} = \frac{Y_k . d . H . J . h^3 . t}{30 \times 10^6 \times K} \text{ inches.}$$

If now we put $Y_k = 1.1$, $d = 200$, $H = 5$, $J = 4$, $h = 10$, $t = 30$, $E = 30 \times 10^6$ and $K = 100$, then deflection

$$= \frac{1{\cdot}1 \times 200 \times 5 \times 4 \times 10^3 \times 30}{30 \times 10^6} = 0{\cdot}44 \text{ inches.}$$

For circular shafts, Dr. Arthur Morley multiplies the various bending moment diagram depths by $\frac{10^4}{D^4}$, instead of by $\frac{K}{I}$, as we have done for our general case. D is the shaft diameter in inches. In this case, for steel circular shafts, we get maximum deflection

$$= \frac{Y_k . d . H . J . h^3 . t}{1475 \times 10^7} \text{ inches.}$$

It is perhaps well to add that the deflection method of Figs. 4 to 6 inclusive is that given publicity in Prof. Goodman's "Mechanics Applied to Engineering" (1st edition); while for much of the later matter the writer is indebted principally to various published work of Dr. Arthur Morley.

There are in most engineering pocket-books handy tables of I's for the more common sections, covering large ranges of sizes. For

this reason, even for circular shafts, the writer prefers the slight modification to Dr. Morley's method which has been outlined.

The squared paper method is not so readily applicable here, or in the example to follow, as in the much simpler case we have already considered. A man really expert at the work might employ it to advantage, but all others should follow the beaten track.

It will be found that with practice, however, part of the construction work can easily be omitted. The derived section figures of Fig. 17 are but the graphical recording of calculations already made. By tabulating in convenient form the various area products obtained, we have all we require at this stage. A man only needs that engineer's *alter ego*, the slide rule, and he can, from the resultant calculated areas, directly plot his results (to t square inches per inch) down the vertical of Fig. 21.

In illustration of the foregoing, let us accord to the various figures the following numerical values :—

I (Fig. 7).	Fig. 9. Bm. depths.	Mid area depths.	Bm. widths.
		a = ·06″	a = ·19″
I_a, 30 inch^4	ab = ·12″	b = ·195″	b = ·22″
$I_b = I_e$, 40 inch^4	be = ·27″	e = ·295″	e = ·125″
I_f, 55 inch^4	ef = ·32″	f = ·38″	f = ·29″
$I_g = I_j$ 80 inch^4	fg = ·44″	g = ·465″	g = ·14″
	gj = ·49″	j = ·5″	j = ·165″

and let K = 100 inch^4.

The above, while not completing the whole range of values, will be quite sufficient to exemplify the procedure.

We have to determine the vertical depths (a) to (j) of Fig. 21. The suggestion is to dispense altogether with the intermediate or derived figure diagram, Fig. 17. The explanation is doubtless unnecessary to many readers ; to some it may be welcome.

We know that the depth (a) (or 1 to 2) of Fig. 21

$$= \frac{\text{Area of derived triangle } a \text{ (Fig. 17)}}{\text{Scale } t}$$

Think a moment. It is surely clear that we do not need to construct that triangle at all. In order to do so, we first multiplied the ordinate ab of Fig. 9 by $\frac{K}{I_a}$. The value of this product gave us the enhanced depth of the triangle in Fig. 17. The area of the derived triangle is *width* into *mean depth* = section width × depth at mid-width. Now, instead of drawing the derived figure after the first calculation, then finally working out the new area from the

new construction, *calculate at once and directly the area required, by reference to its ratio to that of the bending moment area itself.* What is done for the one triangle can be accomplished for the complete diagram. We can tabulate our findings quite conveniently in some such way as is here indicated.

	I.	K/I.	Original Area.	Enhanced Area = original Area × K/I.	Enhanced Area/t, where t = ·25 sq. in. per in.	Σ Enhanced Area/t	
a	30	3·333	·06 × ·19 = ·0114	·038	·152	·152	*a*
b	40	2·5	·195 × ·22 = ·0429	·1071	·4284	·4284 / ·5804	*b*
e	40	2·5	·295 × ·125 = ·0369	·0922	·3688	·3688 / ·9492	*e*
f	55	1·82	·38 × ·29 = ·1101	·2005	·802	·802 / 1·7512	*f*
g	80	1·25	·465 × ·14 = ·065	·0813	·3252	·3252 / 2·0764	*g*
j	80	1·25	·5 × ·165 = ·0825	·1031	·4124	·4124 / 2·4888	*j*
					2·4888		

The final column gives all the data we need for marking off the vertical of Fig. 21. Thus 1 to 2 = ·152″, 1 to 3 = ·5804″, 1 to 4 = ·9492″, and so on till 1 to 7 = 2·4888″. The remaining depths would be similarly negotiated. The advantage of recording the progressive summations is that one can mark all the divisions at one setting of the rule. Place the top of the rule at position 1, and it is very easy to plot points 2, 3, and thus to 13, without any readjustment at all. Such things as these may appear trivial matters; yet they do without doubt appreciably lessen the detail work.

Yet another labour-saver is to be found in the economy possible in the construction work of the ray polygon itself. Here examine Fig. 21a and compare it with Fig. 21. It must be quite obvious that, having clearly marked the various points 1 to 13 inclusive down the vertical, and also the polar point V, all has been done in that diagram which is really necessary for continuing and completing the construction work of the resulting link polygon, Fig. 22. The rays of Fig. 21 are redundant so far as the informed and careful

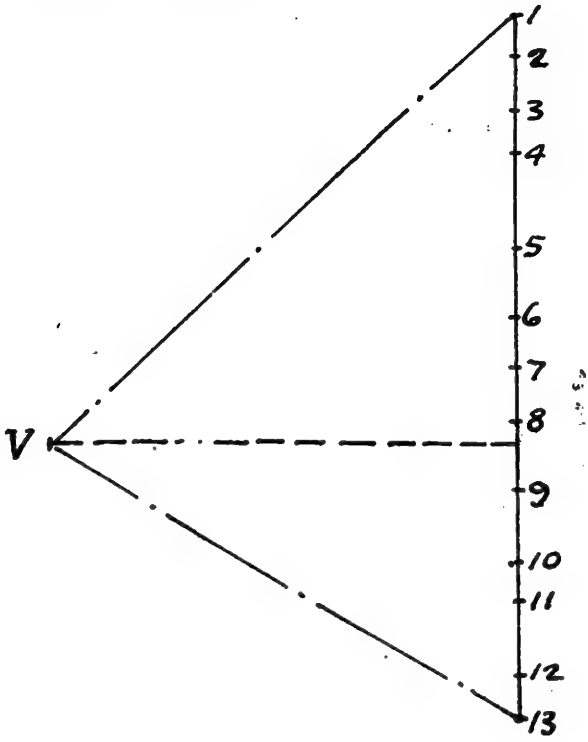

Fig. 21a.

worker is concerned. He simply places tee-square and adjustable square so that the required angle of the latter is related correctly to the polar point and the relevant point in the vertical. He thence proceeds to draw the corresponding deflection diagram link. Obviously great care must be exercised in marking the points and no less care taken in plotting therefrom the deflection links. A further practical caution may be welcomed by the inexpert. See that the tee square blade is not only straight, but that it makes a good firm joint with the tee-head. Any slackness at the joint is ruinous. Also, be sure that the adjustable square maintains its given angles. That, too, is most necessary. A good practice—and one involving no appreciable expenditure of time—is to check each angle on the return journey. It means that as the adjustable is referred back to the ray polygon for its next setting, it is first re-applied to the ray just copied. If there is any disparity, the angle must have been altered somehow. Then is the time to correct the defect. Yet another point—clinographs or adjustable squares with bevelled edges are strongly recommended. Shadows thrown

by thick edges are most annoying and militate against the accuracy required. Where possible, too, train the light on to the working side of the square.

A hint, and briefly, as to the development of the formula; this which we have just considered is but a special application of the previous case for the uniform beam. There, however, E. I. was constant, while here I is variable, though E remains constant. Fig. 9 gives us the bending moment diagram. We now need a suitable provision for each $\frac{\text{Bm. area}}{\text{I}}$ element. Take any depth of Fig. 9, and the Bm. there varies as that diagram depth. We must then divide this depth by I or, what is the same thing, multiply it by $\frac{1}{\text{I}}$. For most values of I, however, this for graphical purposes would make the product unworkably small. Thus we multiply our expression by K, where K is generally not less than the maximum value of I.

As in the previous case considered, 1 square inch of Bm. diagram represents $d.$ H. h^2 lb. inches^2. Now every 1″ on vertical of Fig. 21 = t square inches, and t square inches give $t.$ $d.$ H. h^2 lb. inches^2.

The deflection diagram as constructed is built upon enhanced values resulting from our use of the $\frac{\text{K}}{\text{I}}$ factors. But for this, Y″ depth of the deflection diagram would represent $\frac{\text{Y.}\ (t.\ d.\ \text{H.}\ h^2)\ \text{J.}\ h}{\text{E. I.}}$ inches.

As it is, however, we have $\frac{\text{K}}{\text{I}}$ times that amount, so to right matters we divide the expression by $\frac{\text{K}}{\text{I}}$ or (the same thing) multiply it by its reciprocal. Thus maximum deflection at Y_k

$$= \left(\text{Y}_k \frac{t.\ d.\ \text{H.\ J.}\ h^3}{\text{E. I.}}\right) \frac{\text{I}}{\text{K}} = \frac{\text{Y}_k.\ t.\ d.\ \text{H.\ J.}\ h^3}{\text{E. K.}} \text{ inches.}$$

Where the tabular method just elaborated is adopted, K can, if desired, be incorporated in t; but the formula must be altered accordingly. In order to avoid pitfalls it is probably well to retain K in any case.

At this point a digression may repay us. In what has been already considered we have seen how vital a part the factor I plays. For regular sections, such as circles and rectangles, I (bending)

values have been tabulated covering most one is likely to require. In any case the formulae are readily remembered, *e.g.*, $\frac{\pi}{64} D^4 \text{inch}^4$, for circular beams, where D = diameter in inches; $\frac{B.\ D^3}{12} \text{inch}^4$, for rectangular beams, where B = breadth, D = depth, each in inches. The reader should particularly notice that these I values are those used for bending, not the polar I values used where torque (twisting) is in question.

A set of curves for round sections and another for oblong sections would bridge the gaps one finds in tabulated data. Since I varies directly as the breadth of a rectangular beam, we need only plot values for 1 in. breadth, and for variations therefrom multiply the result by the amount involved.

In figures 10 to 16, however, examples of three different approximate methods are given (two of them graphical) for obtaining I values. Figs. 10, 15 and 16, are two instances of one method. Figs. 11 to 13 illustrate a different treatment; and Fig. 14 illustrates a method whence solution is by approximate formulae. The

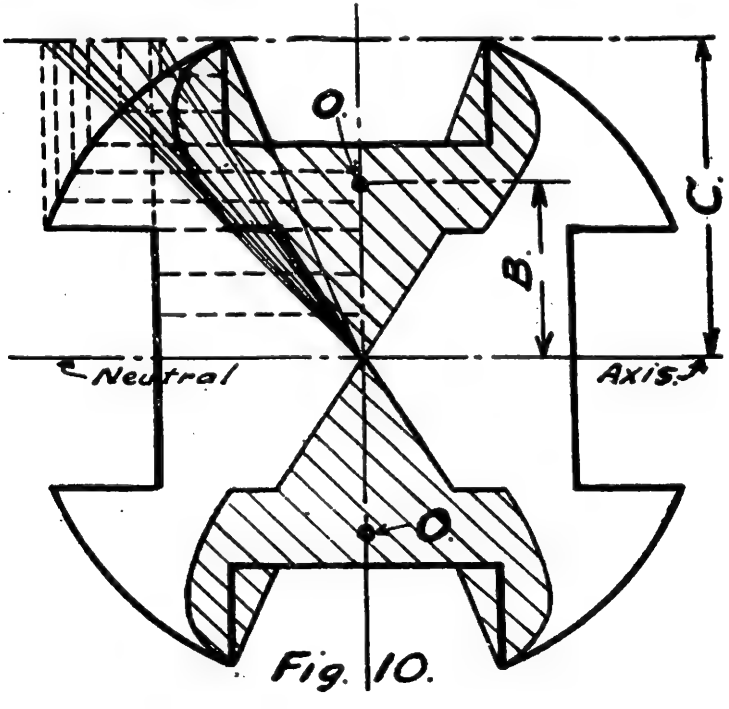

Fig. 10.

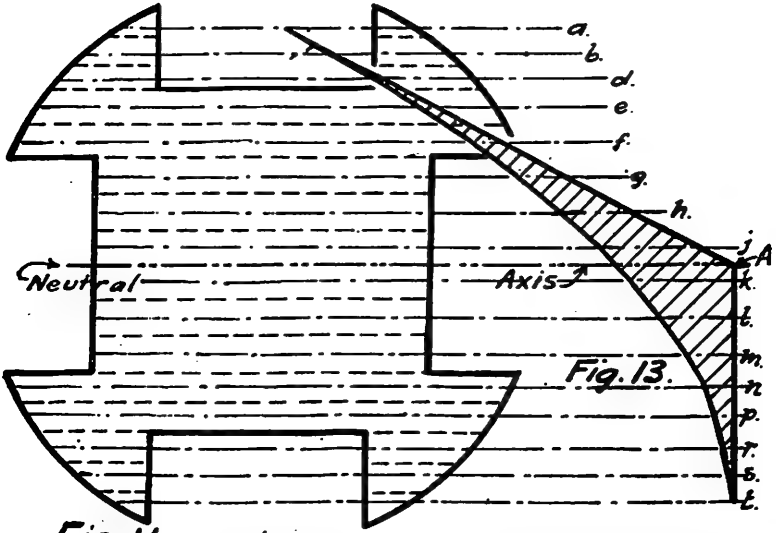

Fig. 11.

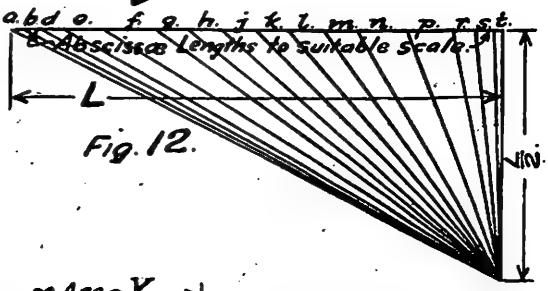

Fig. 12.

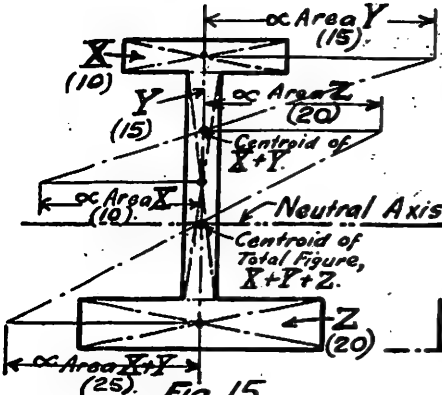

Fig. 15.
(To obtain Centroid).

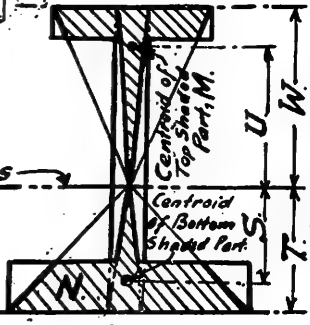

Fig. 16.

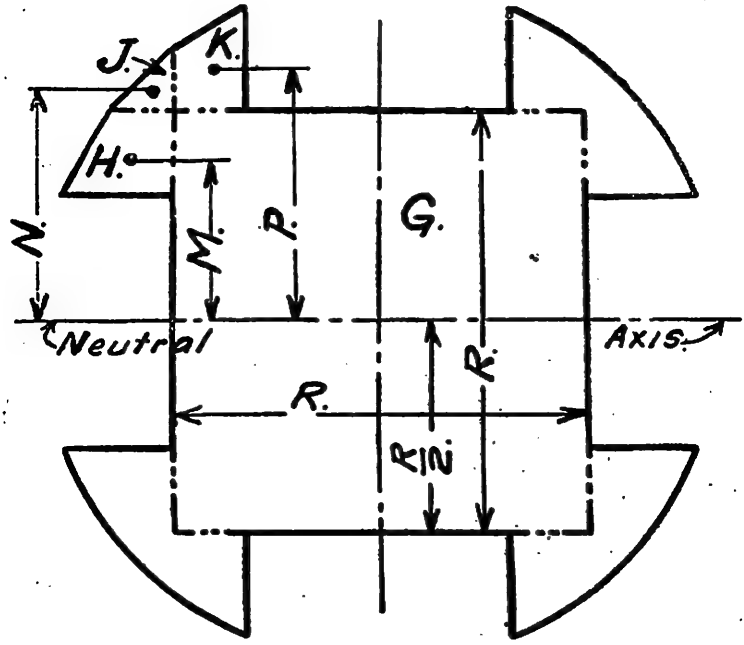

Fig. 14.

big thing is to judge each case on its own merits, and to act accordingly. For the sections shown in Figs. 10, 11 and 14, Fig. 14 provides the shortest cut, and is sufficiently accurate. In each case the figure should be drawn full size.

Fig. 10 is a symmetrical figure—accordingly the neutral axis passes through its geometrical centre. We split up the full size section into a number of horizontal layers (see dotted lines in top left-hand quadrant). At the extreme upper confines of the figure draw a line parallel to the neutral axis. Put the vertical distance between the two lines as C inches. The limit line is shown chain dotted. Where each dotted abscissa intersects the figure outline, project upwards a vertical (dotted) to meet the chain dotted limit line. Then from the centre of gravity of the figure draw a line radiating to each such projection on the horizontal limit. Now mark clearly the point where each horizontal dotted line is intersected by its own exclusively derived ray. Then join up the points thus obtained, and we get the design mapped out in thick outline and cross hatched. Omitting the detailing, the outline has been completed in each of the remaining quadrants. Next ascertain and mark the centroid of the upper shaded area—call it O. This

is, say, B inches above the neutral axis, and similarly O of lower shaded area will be B inches below it.

Let D = area in square inches of each of the two shaded figures, then

$$I \text{ of the total figure} = 2 \times D \times B \times C \text{ inch}^4.$$

No attempt is made to prove this or succeeding statements; but they can be readily checked by comparison with results obtainable otherwise.

Fig. 16 is an entirely different type of section subjected to the same method of treatment. Our first consideration, because the neutral axis passes through it, is to determine the position of the centroid. Since the section is unsymmetrical about one axis, we attack the problem in detail. Refer here to Fig. 15. The C.G. of top flange X is at the point where its diagonals cross; similarly Y's C.G. is at the intersection of Y's diagonals. The vertical centre line of the beam passes through both centroids. We draw a right-handed horizontal whose origin is the C.G. of X, and whose length is proportional to the area of Y. From Y's C.G. we draw a left-handed horizontal proportional in length to the area of X. Join the extremities as shown, and where the diagonal cuts the vertical, we have the resultant C.G. of the top flange and web. Now from this C.G. project a right-handed horizontal proportional in length to area of Z, and draw yet another left-handed horizontal from C.G. of Z in length varying as the areas of X + Y. The diagonal joining these extremities crosses the vertical centre line at the centroid of the total section. As already stated, a horizontal drawn through this C.G. is also the neutral axis of the figure. Now, if :—

Area of top flange	=	10	square inches.
,, web	=	15	,, ,,
,, bottom flange	=	20	,, ,,

then

Arm from C.G. of	X	is proportional to		15,
,, ,,	Y	,,		10,
,, ,,	X + Y	,,		20,
,, ,,	Z	,,		10 + 15 = 25.

The I of the complete full-size section = I of part above neutral axis + I of part below neutral axis;

$$\therefore \quad I = (M.U.W.) + (N.S.T.) \text{ inch}^4, \text{ where}$$

M	=	area, in square inches, of top shaded part,
N	=	,, ,, ,, bottom shaded part,
U	=	distance, in inches, from neutral axis to C.G. of M.,
S	=	,, ,, ,, ,, C.G. of N,
W	=	,, ,, ,, ,, top flange limit,
T	=	,, ,, ,, ,, bottom ,, ,,

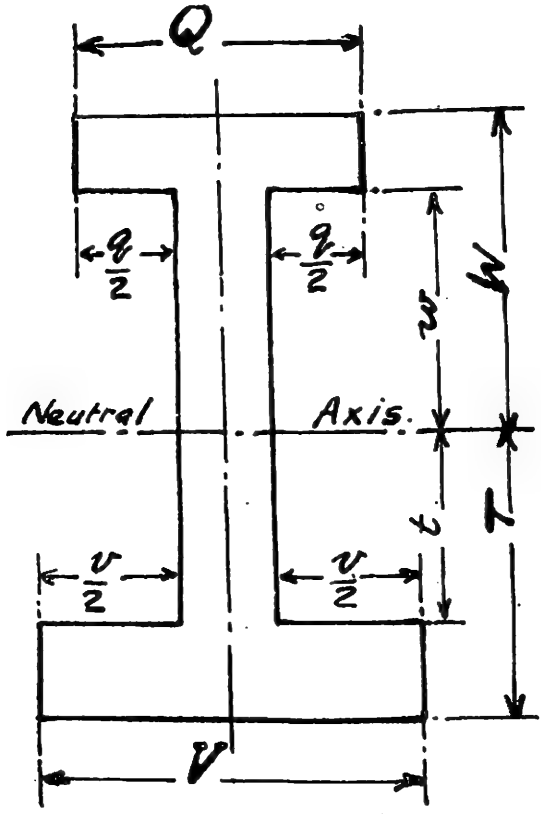

Fig. 16a.

The calculated I for such a relatively simple shape is an easy matter. Refer to Fig. 16a. The various dimensions being in inches,

$$I = \frac{1}{3}\left[(Q.\ W^3 - q.\ w^3) + (V.\ T^3 - v.\ t^3)\right] \text{ inch}^4.$$

We proceed on very different lines in our treatment of Figs. 11 to 13. Split up Fig. 11 into a number of horizontal strips—to ensure greater accuracy of result the more the better. Through each strip C.G. draw an abscissa. These horizontals are shown chain dotted, and are lettered *a* to *t* respectively. Now draw (Fig. 12) a horizontal of length L, and from its right-hand extremity drop a vertical half L long. Then mark off L into sections corresponding in number to, and respectively varying in length as the abscissae *a* to *t* of the beam section, Fig. 11. It will be noticed that the abscissae *a*, *b*, *d*, *r*, *s* and *t* are each comprised of two lengths

bounded by the figure confines. The remaining horizontals are single length lines determined also by the section limits. Now join the various points on the horizontal of Fig. 12 to the lower limit of its vertical.

From the rays of Fig. 12 and the projected horizontal centres of Fig. 11 we are able to construct our link polygon, Fig. 13. Our procedure is very similar to that already described in the previous beam examples. Thus, of the various links, *a* to *b* is parallel to the second ray (that between spaces *a* and *b*) of Fig. 12, and link *s* to *t* of Fig. 13 is parallel to ray nearest vertical of Fig. 12. The two lines in Fig. 13 drawn parallel to the first and last rays respectively of Fig. 12, and meeting in A, complete the final link polygon. The heavy dot and dash horizontal passing through junction A is the neutral axis of the section.

Then $I = E \times F$ inch^4, where

E = area in square inches of total full-size section (Fig. 11).
F = ,, ,, ,, shaded diagram (Fig. 13).

For assessing area values of irregular figures, it is often well to work by Simpson's rule, or else to use a planimeter.

It is sometimes rather troublesome to determine with reasonable accuracy the position of the centroid. If the figure lends itself to dissection into more or less regular forms, then the problem can be attacked in detail on lines similar to those described for Fig. 15. In any case a person familiar with the use of the planimeter can usually find a solution without undue difficulty or grave error. The centre of gravity is, of course, at the intersection of axes which are at right angles to each other. It is necessary therefore to locate each axis. Where a figure is only non-symmetrical about one axis, the work is practically halved. Let us assume the figure wholly without symmetry, however. We can generally tell *by inspection* the *approximate* position, say the *x x* axis should occupy in order to divide the figure through its centre of gravity. Accordingly, we draw in the line *x x where we think it should be.* We next obtain the area of each part by planimeter or other means, and also guess as closely as possible the position of the respective centres of gravity of the two sub-areas. For the line *x x* to be rightly placed, the one "sub-area into distance" *moment* must equal the other. Usually the disparity between the two moments will be found to be very small. It will be evident at once whether the line *x x* has to be removed slightly to the one side or the other. Now, obviously the amount of adjustment is calculable within close limits. The element of area removed from one part is taken over by the other part. For so narrow a slice it is easy to estimate the *average* length. Let *l* be the length and δw the width. Accordingly, $l \times \delta w$ is added to the area of the smaller part and subtracted from the larger, while the arm (the leverage) of the former is increased

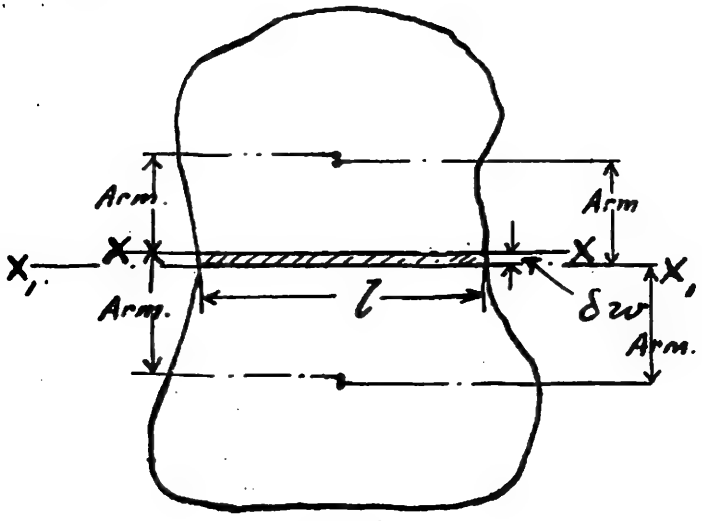

Fig. 16b.

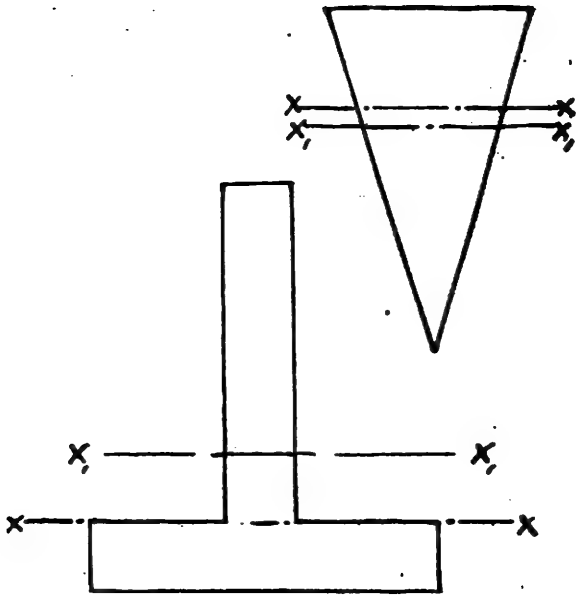

Fig. 16c.

approximately by $\frac{1}{2}\,\delta\,w$ and the arm of the latter is reduced approximately by $\frac{1}{2}\,\delta\,w$. That provides an equation whence solution is readily obtainable in terms of $\delta\,w$. Again, a close guessing of the value of $\frac{1}{2}\,\delta\,w$, for addition to and subtraction from the respective leverage arms, will simplify the expression. In any case it will be found that $(\delta\,w)^2$ cancels out. Once $\delta\,w$ has been obtained, the required centre of gravity is to be found in a second axis removed approximately $\delta\,w$ from $x\,x$ (see $x_1\,x_1$ of Fig. 16b). All this, which has taken too long in description, is really quite simple and fairly quick work once seriously tackled. What has been done for the one axis must be also done for the other axis normal to the first. The centre of gravity is at, or very near to, the intersection of these approximated axes. The reader should specially note that the centre of gravity does not necessarily lie upon a line dividing the area into halves. It is in the *balancing* centre, whence *moments* to the one side and the other are equal. The two sections of Fig. 16c, for instance, illustrate this difference in the cases of a tee and a triangular section respectively. The line $x\,x$ divides the areas equally, the line $x_1\,x_1$ contains the centre of gravity. The axes coincide in such cases as squares and rectangles. This difference was overlooked at this juncture in the first revised issue of the pamphlet.

In lieu of the planimeter method, one can readily combine Simpson's rule and the principles underlying Fig. 15. The resulting hybrid will prove a thriving growth. Thus, divide the area to be treated into a number of horizontal strips of equal height. If the strip widths from the base upwards be a, b, c, d, etc., and the heights be h, then the areas are respectively ah, bh, ch, dh, etc. Now by reference to the horizontal base line, the various leverage arms are approximately :—

$$\frac{h}{2}\quad\frac{3h}{2}\quad\frac{5h}{2}\quad\frac{7h}{2}\ \text{etc.}$$

Then the height H (for axis required)

$$= \frac{ah\,\frac{h}{2} + bh\,\frac{3h}{2} + ch\,\frac{5h}{2} + dh\,\frac{7h}{2} + \text{etc.}}{ah + bh + ch + dh + \text{etc.}}$$

$$= h^2\,\frac{(\cdot5a + 1\cdot5b + 2\cdot5c + 3\cdot5d + \text{etc.})}{h\,(a + b + c + d\ \text{etc.})}$$

$$= h\,\frac{(\cdot5a + 1\cdot5b + 2\cdot5c + 3\cdot5d + \text{etc.})}{a + b + c + d + \text{etc.}}$$

In general terms we can state, $\text{H} = \dfrac{\Sigma\,(\text{Areas} \times \text{mean heights})}{\Sigma\ \text{Areas}}$

We repeat the procedure in order to obtain the vertical axis; and the centroid is located where the two axes intersect.

The final method here indicated has in the case of the fairly simple section chosen (Fig. 14) much to recommend it. The neutral axis in this case coincides with the horizontal centre line. The inscribed square G, as we can see, is by far the largest part of the figure, and its $I = \frac{1}{12} R^4$ inch^4, where R is the length of each side in inches. Now, considering the top left-hand quadrant, the external portion still to be treated can be subdivided into areas H, J and K. Replacing the outer arc by suitable chords, we get two equal trapezia and a triangle. Determine the areas (in square inches), and mark their centroids. Then the I of H about the neutral axis = approximately $H \times M^2$ inch^4, I of J = approximately $J \times N^2$ inch^4, and I of K = approximately $K \times P^2$ inch^4, where M. N. and P are respectively vertical distances (in inches) separating the various gravity centres and the neutral axis. To this, strictly speaking, we ought to add the I of each such element about its own axis. Such additions as are here considered are usually so small by comparison that, except where extreme accuracy is needed, they are scarcely necessary for ordinary working calculations. In any case it is near enough to give the I's for roughly equivalent triangles and rectangles respectively. Thus, the I for a triangle about its neutral axis is $\frac{1}{36} b h^3$ inch^4, and for the rectangle about its neutral axis is $\frac{1}{12} b h^3$ inch^4, where in each case b is the base (or width) and h the height, dimensions being in inches.

To resume, since there is an H, J, and K area system in each quarter of the figure, the approximate total I of the section = I of inscribed square + I of each external part about the neutral axis.

$$\therefore \text{ approx. } I = \frac{I}{12} R^4 + 4 [(H M^2 + J N^2 + K P^2)] \text{ inch}^4$$

Of course the more we sub-divide the external areas, the nearer we approach the correct result. It might be added also that with a symmetrical figure, whichever angle of rotation we give it, the I remains constant—this, however, does not obtain for unsymmetrical sections, nor does it apply to the Z of non-circular sections.

As a slight variant to the treatment just described, it is at times preferable to take the *difference between the* I *of the figure as uncut and that of the cut-away portions.* The writer has found this to be an advantage when dealing with the slotted body part of a one-piece combined rotor body and shaft for turbo alternators.

Figs. 19 and 20 show a triangle and trapezium, and indicate the method of obtaining centre of gravity and area of each.

4. We now make our final effort. It may prove a somewhat tedious undertaking, but should be less difficult than lengthy. The

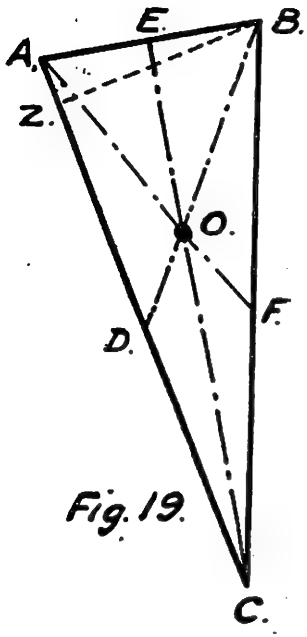

Fig. 19.

D bisects CA,
E " AB,
F " BC.

O, where AF, BD, & CE intersect, is the Centroid of the Triangle.

BZ is normal to CA.

Area of Triangle = BZ × DA.

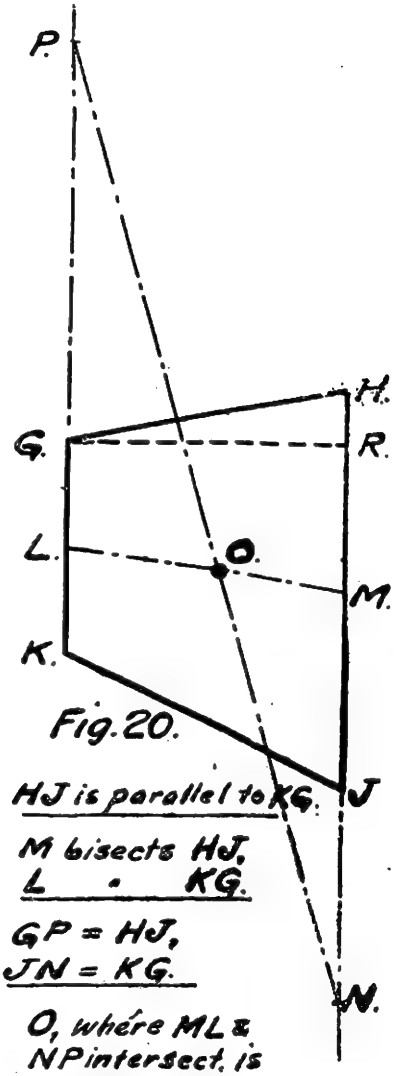

Fig. 20.

HJ is parallel to KG.

M bisects HJ.
L " KG.

GP = HJ,
JN = KG.

O, where ML & NP intersect, is the Centroid of the Trapezium.

GR is normal to HJ & KG

Area of Trapezium = $GR \times \left(\frac{HJ + KG}{2}\right)$

explanations already given lessen appreciably the descriptive work still necessary.

Let us consider, then, the reactions at supports, bending moments, and deflections of a variable section beam freely supported at outer ends, spanning four unequally pitched supports, and subjected to unequally spaced, constant, concentrated, and dissimilar loading, fixed lengthwise between supports.

First, we draw in the beam length to scale, showing varying sections of beam and relative positions of supports and impressed loads. Fig. 23 gives us the system.

The procedure we shall adopt is a particular application of an ingenious and simple method to which the late Dr. George Wilson gave welcome publicity in 1897.

Our initial step is to treat the beam as loaded, *i.e.*, under action of loads BC, CD, DE, EF and FG, *but as supported at the ends only*. In other words, at this stage we ignore the prop reactions altogether. Fig. 24 illustrates this, the prop positions being marked in dotted triangles. The required ray polygon is Fig. 25, and Fig. 26 gives the resultant link polygon. Then follow our enlarged area figures of Fig. 27, consequent upon them ray polygon, Fig. 28, and finally from Figs. 27 and 28 our first tentative deflection diagram, as shown in Fig. 29. All this is, of course, merely a repetition of methods already described.

Now scale the depth of this diagram at each prop centre ordinate —that at right-hand centre is lettered *a*, at left-hand centre *b*. These depths *a* and *b* are proportional to the deflections of the beam at the prop centres *when the props are lowered below the contour of the bent beam so as not to touch it.*

It is well before we proceed further to fix clearly in our minds what it is we are really seeking to do. We are assuming, of course, that the complete system is one in which the supports and props are all in equal vertical alignment. Thus it is obvious that the deflections occur between the support and prop centres, while at those centres they are nil. So far as we have gone, treating the beam as not propped up at all, we get deflections *a* and *b* at the axial positions corresponding to the respective prop centres. We must now cast about for a means to discover what reaction load R at right-hand prop and S at left-hand prop (see also Fig. 48) will so thrust up the beam that deflections *a* and *b* just vanish. In other words, *a* and *b* must each equal precisely nothing. This done, if we have not made the harbour, we have at all events crossed the bar; and the rest is plain sailing, mostly repetition work. It is no short cut, but to those who are interested it is decidedly interesting work. It is the sort of thing for the best kind of "wait and see" man. It is often the "wait and see" men who are the true "do it now" breed. So long as a "wait and see" policy is not the negative vice of indolence, but the positive virtue of research, it

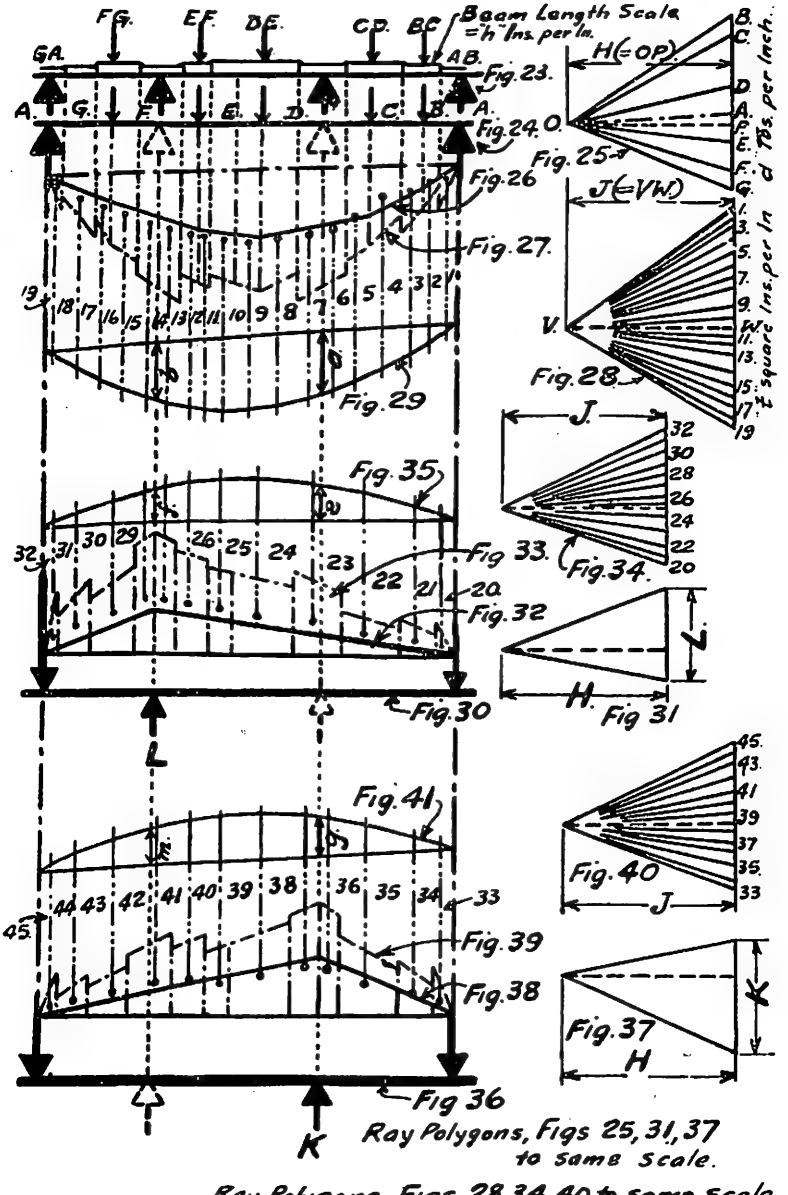
Beam Length Scale = h" Ins. per In.
H(=OP)
J(=VW)
1" Square Ins. per In. of Lbs. per Inch.
Fig. 23.
Fig. 24.
Fig. 25.
Fig. 26
Fig. 27.
Fig. 28.
Fig. 29
Fig. 30
Fig. 31
Fig. 32
Fig. 33.
Fig. 34.
Fig. 35
Fig. 36
Fig. 37
Fig. 38
Fig. 39
Fig. 40
Fig. 41
Ray Polygons, Figs 25, 31, 37 to same Scale.
Ray Polygons, Figs. 28, 34, 40 to same Scale.

exemplifies the true spirit of science; and art, wisely led, will follow on apace.

The reader should recall that deflection varies directly as the loading. Thus, if we have a certain deflection curve for one specified load, by doubling that load and keeping to the same scales throughout, we get a curve whose ordinate depths are all likewise doubled. Similarly for a second load, and any number of loads. We treat each individually and then summate their values at any point desired. This, by the way, is what we have already done, but we have journeyed by a different route.

We now *assume* a value (any value we like) for the reaction load acting upwards at the left-hand prop position. Call it L, as per Fig. 30. We find how much L reduces the deflection at each prop centre. Next we try the effect of another assumed reaction load K (Fig. 36) acting upwards at the right-hand prop position, and see what deflection reduction this produces at each prop centre. Specially notice that we treat the two cases apart. This done, we have in our hands a key to release our lock.

Next, then, in Figs. 30 to 35 inclusive, we work out our second stage. As in the preceding sequence we neglected the prop reactions, here we ignore the effect the loads have upon the beam. *We now treat the system as a beam freely supported at ends and subjected to one upward load* L *alone, at left-hand prop centre.* Thus the end support reactions are considered as downward forces. Fig. 30 represents the loading system, Fig. 31 is first ray polygon, bending moment diagram is to Fig. 32, and derived area figures make up Fig. 33. From Fig. 33 we get second ray polygon Fig. 34, and thence by means of both we are able to conclude the series in deflection diagram, Fig. 35. Specially take note, *for it is most important,* in this and the succeeding series of figures, the various scales must coincide with those chosen in the first sequence. We now scale the second deflection diagram heights at each prop centre. The right-hand height is *e*, the left-hand *f*.

Next repeat this procedure, but for the assumed load K at the right-hand prop centre. Thus we obtain Figs. 36 to 41, of which link polygon, Fig. 41, is the deflection diagram. Again scaling diagram heights, *g* is that at the right-hand, and *m* that at the left-hand centre.

Being now furnished with the various deflection values, *e.g.*, *a* downwards as opposed by *e* and *g* upwards, and *f* and *m* upwards against *b* downwards, we possess all the necessary data for solving our problem. Figs. 42, 43, also 44, 45 and 46, 47 summarise our labour of love, or if we prefer it so, our act of penance.

Recall that the tentative load L (Fig. 44) produces a deflection *f* against *b* and *e* against *a*. Assumed load K (Fig. 46) gives *m* opposed to *b* and *g* to *a*. We now require S, the actual load at the left-hand prop, and R, the actual load at the right-hand prop,

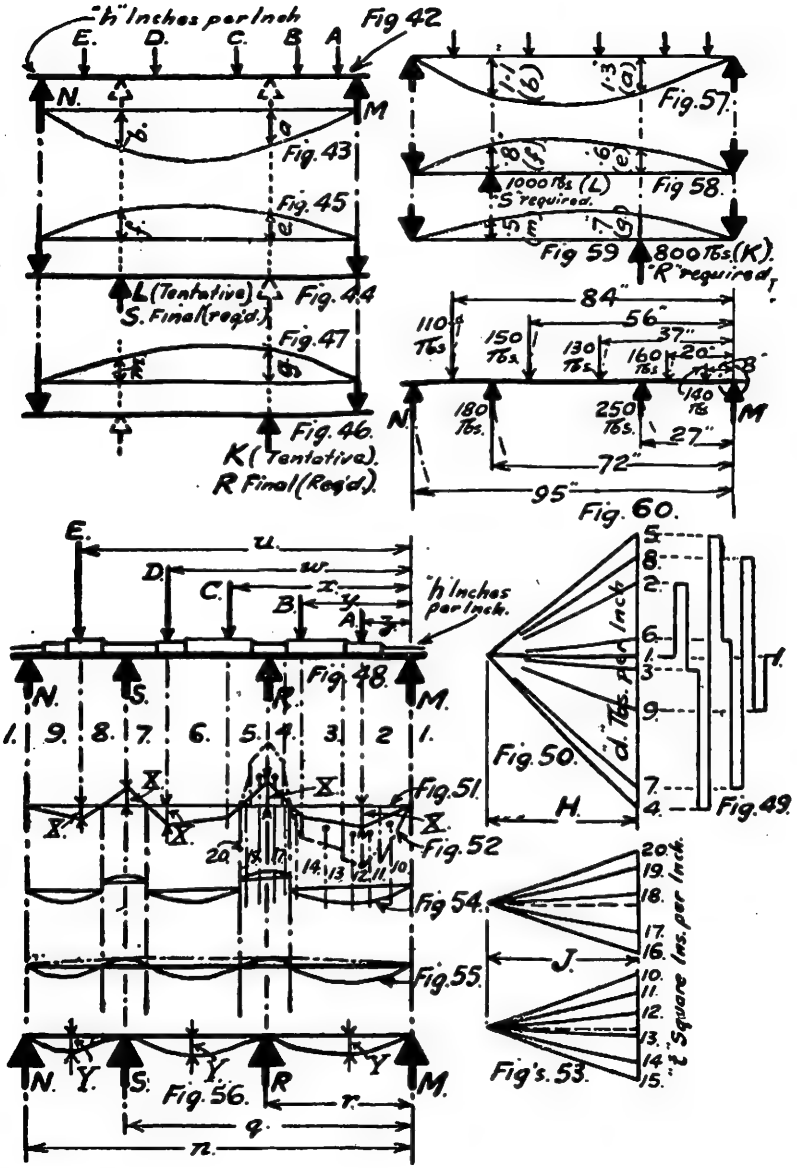
"h" Inches per Inch
Fig 42
E. D. C. B A
N. M
Fig. 43
Fig. 45
L (Tentative)
S. Final (req'd.)
Fig. 44
Fig. 47
Fig. 46.
K (Tentative).
R Final (Req'd.)
Fig. 57.
1000 lbs. (L)
S required.
Fig 58.
Fig 59
800 lbs. (K).
R required.
84"
56"
37"
20"
110 lbs
150 lbs
130 lbs
160 lbs
140 lbs
180 lbs.
250 lbs.
27"
72"
95"
Fig. 60.
E. D. C. B A
u. w. x. y. z.
"h" Inches per Inch.
Fig. 48.
N. S. R. M.
1. 9. 8. 7. 6. 5. 4. 3. 2. 1.
Fig. 51.
Fig. 52
Fig 54.
Fig. 55.
N. S. R. M.
Fig. 56.
r.
q.
n.
Fig. 50.
H.
Fig. 49.
"h" Inches per Inch
"I" Square Ins. per Inch.
J.
Fig's. 53.

whose joint reactions exactly nullify the deflections b and a at the prop centres.

Consider deflection at right-hand prop centre. Downward deflection a due to loads A to E inclusive is reduced by upward deflection g due to K.

Thus if K lbs. gives g inches, 1 lb. gives $\frac{g}{K}$ inches, and R lbs. $R\frac{g}{K}$ inches.

But a is also reduced by upward deflection e due to L.

Thus also if L lbs. produces e inches, S lbs. gives $S\frac{e}{L}$ inches.

Next, take deflections at centre of left-hand prop. Here downward deflection b due to loads A to E inclusive is reduced by upward deflection f due to L.

Thus L lbs. gives f inches, and hence S lbs., $S\frac{f}{L}$ inches.

Again b is also lessened by upward deflection m due to K.

So K lbs. produces m inches, and R lbs., $R\frac{m}{K}$ inches.

When supports and props are all at the same level, the upward deflections exactly equal the downward deflections.

Therefore, summarising the foregoing, at right-hand prop,

$$R\frac{g}{K} + S\frac{e}{L} = a \qquad (2)$$

At left-hand prop, $R\frac{m}{K} + S\frac{f}{L} = b$ (3)

Now cross multiply: (2) by m; (3) by g.

$$\text{Then } R\frac{gm}{K} + S\frac{em}{L} = am$$

$$\text{and } R\frac{gm}{K} + S\frac{fg}{L} = bg$$

$$\text{Subtract, then } S\left(\frac{em - fg}{L}\right) = am - bg;$$

$$\therefore \quad S = \frac{L(am - bg)}{em - fg} \text{ lbs.}$$

To obtain R, multiply (2) by f, (3) by e.

$$\text{Then } S\,\frac{ef}{L} + R\,\frac{fg}{K} = af,$$

$$\text{and } S\,\frac{ef}{L} + R\,\frac{em}{K} = be$$

$$\text{Subtract, then, } R\left(\frac{fg - em}{K}\right) = af - be;$$

$$\therefore \quad R = \frac{K\,(af - be)}{fg - em} \text{ lbs.}$$

In illustration of the foregoing, if we accord to the various diagram ordinates the numerical values shown in Figs. 57 to 59, we get :—

$$R = \frac{K\,(af - be)}{fg - em} = \frac{800\,[\,(1{\cdot}3 \times {\cdot}8) - (1{\cdot}1 \times {\cdot}6)\,]}{({\cdot}8 \times {\cdot}7) - ({\cdot}6 \times {\cdot}5)}$$

$$= 800 \times \frac{{\cdot}38}{{\cdot}26} = 1170 \text{ lbs.};$$

$$\text{and } S = \frac{L\,(am - bg)}{em - fg} = \frac{1000\,[\,(1{\cdot}3 \times {\cdot}5) - (1{\cdot}1 \times {\cdot}7)\,]}{({\cdot}6 \times {\cdot}5) - ({\cdot}8 \times {\cdot}7)}$$

$$= 1000 \times \frac{-{\cdot}12}{-{\cdot}26} = 462 \text{ lbs.}$$

Probably a quicker way of obtaining S here would be to substitute value of R in expression (2) thus :—

$$R\,\frac{g}{K} + S\,\frac{e}{L} = a;$$

$$\therefore \quad \left(1170 \times \frac{{\cdot}7}{800}\right) + \left(S \times \frac{{\cdot}6}{1000}\right) = 1{\cdot}3;$$

$$\therefore \quad {\cdot}0006\,S = 1{\cdot}3 - 1{\cdot}023 = {\cdot}277;$$

$$\therefore \quad S = 462 \text{ lbs.}$$

Having now fixed up the prop reactions, those for the two supports follow very readily. The great thing to remember is to work from first principles. Thus the beam being in equilibrium, *the sum of the loads exactly equals that of the support and prop reactions.* Further, if we assume the beam as pivoted, say at M, *then the counter-clockwise load moments are precisely balanced by the clockwise reaction moments.* Of course, if we considered the fulcrum as at N, then the load moments would be clockwise and those of the reactions

counter-clockwise. The one set of moments, however, would still exactly balance the other.

Figs. 48 and 56 show the opposing loads and moments. Thus, to obtain reaction load N, we have :—

$$A z + B y + C x + D w + E u = R r + S q + N n ;$$

$$\therefore N = \frac{A z + B y + C x + D w + E u - R r - S q}{n} \text{ lbs. ;}$$

and for M, $A + B + C + D + E = M + R + S + N$;

$$\therefore M = A + B + C + D + E - R - S - N \text{ lbs.}$$

Taking the values shown in Fig. 60,

$$95\ N = (8 \times 140) + (20 \times 160) + (37 \times 130) + (56 \times 150) + (84 \times 110) - (27 \times 250) - (72 \times 180) = 7060 ;$$

$$\therefore N = \frac{7060}{95} = 74{\cdot}5 \text{ lbs., say 75 lbs.}$$

$$M = 140 + 160 + 130 + 150 + 110 - 250 - 180 - 74{\cdot}5 = 185{\cdot}5 \text{ lbs. say 185 lbs.}$$

Perhaps it is well to point out that the loads chosen in Fig. 60 are simply given as illustrations, and are consistent merely as regards the way they total correctly. They have no necessary relation to any actual calculated beam sections or alignment levels.

Having got thus far, the method of obtaining the resultant bending moment diagram for the complete system is one of considerable interest. For it—as for so much else—the writer is indebted to the masterly work of Professor Goodman.

Mark off on the vertical of ray-polygon, Fig. 50, the various loading to a convenient scale. Earlier on we had something to say about notation and sensing. We have here a very neat case in point. Refer to Fig. 48. Reaction M we should call 1, 2. Take any point 1 in vertical of Fig. 50. Since M (in Fig. 48) exerts an upward thrust against the beam, the sensing, as represented by the arrow, is upward. So next we mark point 2 in vertical of ray polygon *above* 1, and distant from it an amount proportional to load M. Thus if M = 185 lbs. and our load scale be 100 lbs. per inch, then 2 is $\frac{185}{100} = 1{\cdot}85''$ *above* 1.

We go *up* from 1 to 2. From 1 draw a pole H normal to the vertical. Next in order on Fig. 48 we get load A acting downwards between 2 and 3. Therefore from point 2 in Fig. 50 we *drop* a distance proportional to load A, and mark the lower limit 3. Likewise B (downwards) is represented on load line of Fig. 50 as *drop* from 3 to 4. So finally N acting upwards in Fig. 48 is shown in vertical of ray polygon by *height* from 9 to 1. This up

and down business is drawn pictorially in Fig. 49. Now specially notice that as our *ups* equal our *downs*, the starting point 1 of Fig. 50 coincides with the finishing point 1. The various steps of Fig. 49 are projected horizontally on to the vertical of the ray polygon, and where they impinge, these points are joined to the remote end of pole H.

We now complete our link polygon series of Fig. 51. Starting in space 2 we draw a line across it parallel to ray 2 of Fig. 50. Continuing, we join the first link by another stretching across space 3, this being in turn parallel to ray 3. So we proceed till space 9 is crossed by link parallel to ray 9 of Fig. 50. Finally our resultant line joining the diagram extremities is parallel to the horizontal marked 1 in the ray polygon. Incidentally this provides us with an important check upon our construction work. Thus, if the resultants of the two figures are not parallel we have gone astray somewhere, and it is up to us to discover where the error lies. Resuming, we have in Fig. 51 our final bending moment diagrams. There are three positive (downward) diagrams, and two negative (upward) diagrams.

One method—and probably the simplest and most direct—of determining the resultant deflections throughout the entire system, is by a corrected summation procedure. It is very conveniently arranged in tabular form, as indicated below. The great thing to remember is that we are dealing with the algebraic sum of component deflections. Thus, we have the load deflections of Fig. 43 downwards, the *tentative* prop deflections of Figs. 45 and 47 upwards. Moreover, the corrected prop reactions, S and R, have been calculated. Now, the *resultant* deflections, say at positions A, B, C, D, and E (see Fig. 42) are the algebraic sums of component deflections at those positions. We, therefore, measure the depths of the respective diagrams at the A to E positions. Do not forget, however, that as regards diagrams, Figs. 45 and 47, their depths have to be corrected to accord with the finally calculated values of S and R (in lieu of L and K, upon which the diagrams are based). Thus, the diagram depths (literally here heights) of Fig. 45 are multiplied by $\frac{S}{L}$, while those of Fig. 47 are multiplied by $\frac{R}{K}$. This done, from depth at A, Fig. 43, subtract corrected depth at A of Fig. 45 and corrected depth at A of Fig. 47. The remainder so obtained must now be multiplied by the common scale of all the three deflection diagrams. Then, this product of "scale into algebraic sum" gives the actual resultant deflection required at position A. As with this position A, so proceed and thus obtain the resultant deflections at the remaining positions B to E inclusive. The work can be conveniently arranged in some such manner as immediately follows :—

	LOAD POSITIONS.						
	E	(S)	D	C	(R)	B	A
Depths, Fig. 43	+0·7″	+1·1″	+1·5″	+1·4″	+1·3″	+1·1″	+0·6″
,, ,, $45 \times \frac{S}{L}$	−0·5″	−0·9″	−0·9″	−0·8″	−0·7″	−0·5″	−0·2″
,, ,, $47 \times \frac{R}{K}$	−0·15″	−0·2″	−0·45″	−0·52″	−0·6	−0·5″	−0·35″
Algebraic Sum	+0·05″	(0)″	+0·15″	+0·08″	(0)″	+0·1″	+0·05″
Scale × Alg.Sum = δ	+0·005″	(0)″	+0·015″	+0·008″	(0)″	+0·01″	+0·005″

N.B.—The bracketed S and R data are added, being useful as an extra check on the accuracy of the working, for obviously if the resultant is other than 0 some mistake has been allowed to creep into the calculations. Until that has been rectified, the remainder of the data cannot be accepted. It is, moreover, well to point out that the values given are purely hypothetical. In accordance with accepted conventions, downward pointing diagrams are considered positive, upward-pointing diagrams negative. The assumed scale in this case is one-tenth inch per inch depth of diagrams. That sufficiently explains the summations concerned.

The above method is one the writer almost invariably adopted where several deflection values were required in a multi-support system.

A variant upon the above procedure may be referred to. As it involves additional graphical constructions, it is not recommended for general use. Though these extras take the place of the tabled work just described, the latter is more quickly negotiated. One advantage of the alternative method is that a deflection system, or a span of such a system, can be plotted to a large scale, in a manner and to a degree not readily facilitated by deductions from tabled summations. In order to draw a resultant diagram of say a four-support system, from data provided in the component diagrams, it will be necessary to scale a large number of intermediate positions. Then, also, it has to be remembered that each final figure is proportional to small *differences* of *scaled* depths. Accordingly, the resultant curves will probably have to be accommodated between somewhat irregular individual point markings. On the other hand, in the alternative procedure, depths are very closely proportional to final deflection values, instead of the deflections varying as the differences of scaled depths. That is the justification, if any, for the variant immediately to be described. The additional work entailed, however, is considerable.

Related to the bending moment diagrams of Fig. 51 are the derived figure diagrams, two of which are shown chain-dotted in Fig. 52. The remaining three would be similarly negotiated. The two figures Fig. 53 are the ray polygons based on the diagrams Fig. 52, the lower from the positive, the higher from the negative derived figure. The two right-hand deflection diagrams of Fig. 54 are constructed by reference to Figs. 52 and 53, and the remaining three are obtained in like fashion. Fig. 55 brings these five diagrams into line, whence there still remain three positive and two negative curves. By joining, as shown chain-dotted, extremities to crests and crest to crest, we have three span curves proper, whose amplitudes are measured between new chain-dotted resultants and the relevant depth limits. In Fig. 56 the end diagrams have been tilted so that the chain-dotted line (here the new full-line) is straight throughout the system. This indicates very closely *to scale* the form of the bent beam along each of the three spans. Accordingly, the various depths, as Y, at any position along any span, are proportional to the actual deflections there. They probably yield closer results than those based upon differences between scaled depths. These depths Y, multiplied by "scale," are the deflection values required. Computation of scales for bending moment and deflection diagrams is as already given earlier in the pamphlet.

In the case of certain multiple-support systems, as for electrical machines, it is sometimes accounted good practice to lighten somewhat the reaction loads on the props by a proportionate increase of load on the end supports. This is done by inserting additional liners under the tail bearing pedestals. It is, of course, tantamount to a *lowering* of the intermediate bearings; and that is what is allowed for in the relevant calculations. In the case treated, for instance, R and S would accordingly have been given some lesser value as determined by the amounts the props were lowered or (the same thing) the end supports raised. Generally, under such conditions, however, it is R and S which are given some smaller pre-determined value; and the problem then is to determine the amounts of tail bearing adjustment to suit those prescribed reactions.

In the case of uniform beams this problem of determining prop reaction loads and of deflections is capable of much quicker treatment than by the processes described for beams of variable cross section.

Mr. Livingstone notably, and others before him,* though much less prominently, have given valuable sets of curves which, though they necessitate some slight increase in the mathematics, cut out

* Reference may in this connection be made in particular to Mr. H. Edington's article, "Deflection of Armature Shafts," *Engineering*, January 31st, 1913.

the graphics, and so facilitate a very considerable and desirable saving of time and labour.* This applies, however, only to beams of approximately uniform section, and while for such systems, by enabling us with comparative ease to obtain prop reactions, it saves us also some of our stages in the treatment of multiple support bending moment diagrams, it does not otherwise directly help us in deriving bending moment values themselves. These, and deflections for variable section beams, should be tackled in some such way as just described.

Mr. Ernest Barlow, *vide The Draughtsman* for February and March, 1921, has presented a mathematical treatment for the deflection of a variable section two-support rotor, in his paper entitled "Deflection and Critical Speed of a Turbo Alternator Rotor."

Those interested should read likewise carefully the article on "Simplified Approximations of Critical Speeds," *Engineering*, 25th November, 1921, by Mr. G. Arrowsmith, M.Sc. This article also has reference to variable section two-support systems. Mr. Arrowsmith has boiled down his work most successfully. His claim that results are approximately correct is a diffident one. They have been found to be correct to within 3 per cent. for deflections, and $1\frac{1}{2}$ per cent. for critical speeds, over a fairly wide range of practical sizes, for turbo-alternator rotors. They tend to diverge more where it comes to a case of very long bodies and relatively stubby shaft ends, such as characterise certain largest ratings in 3,000 R.P.M. machines. In one instance the disparity then in critical speed reached some $7\frac{1}{2}$ per cent., the graphical and closer treatment giving the higher value.

And now, doubtless, readers will be relieved that the paper is at an end.

A late parson friend of the writer once said, referring of course to something entirely different : "Those who like this sort of thing, this is the sort of thing they like."

* A.E.S.D. members should not need reminding that there is also an A.E.S.D. chart (published about 1927) which covers the ground adequately in this respect. The present writer, too, quite independently, and not knowing the particular application given in the Association Data Sheet, presented in his article, "Deflection of Uniform-Section Beams," *World Power*, October, 1930, and October, 1931, a diagram which he only discovered in the proof stage to be based substantially on the principle adopted in the A.E.S.D. chart. A foot-note in the article concerned emphasises this point. The writer may perhaps be permitted to add that the article gives the mathematics covering the case of practically any two-support system (including also those with over-hung loading) and by implication, multiple-support systems. It points out, too, possible pitfalls in the use of certain equivalents for stepped beams, by showing their rightful and strictly limited applications.

A.E.S.D. Printed Pamphlets and Other Publications in Stock.

An up-to-date list of A.E.S.D. pamphlets in stock is obtainable on application to the Editor, *The Draughtsman*, 96 St. George's Square, London, S.W.1.

A similar list is also published in *The Draughtsman* twice a year.

Readers are asked to consult this list before ordering pamphlets published in previous sessions.

List of A.E.S.D. Data Sheets.

1. Safe Load on Machine-Cut Spur Gears.
2. Deflection of Shafts and Beams. } Connected.
3. Deflection of Shafts and Beams (Instruction Sheet). }
4. Steam Radiation Heating Chart.
5. Horse-Power of Leather Belts, etc.
6. Automobile Brakes (Axle Brakes). } Connected.
7. Automobile Brakes (Transmission Brakes). }
8. Capacities of Bucket Elevators.
9. Valley Angle Chart for Hoppers and Chutes.
10. Shafts up to 5¼-in. diameter, subjected to Twisting and Combined Bending and Twisting.
11. Shafts, 5¾ to 26 inch diameter, subjected to Twisting and Combined Bending and Twisting.
12. Ship Derrick Booms.
13. Spiral Springs (Diameter of Round or Square Wire).
14. Spiral Springs (Compression).
15. Automobile Clutches (Cone Clutches).
16. ,, ,, (Plate Clutches).
17. Coil Friction for Belts, etc.
18. Internal Expanding Brakes. Self-Balancing Brake Shoes (Force Diagram). } Connected.
19. Internal Expanding Brakes. Angular Proportions for Self-Balancing. }
20. Referred Mean Pressure Cut-Off, etc.
21. Particulars for Balata Belt Drives.
22. ¾" Square Duralumin Tubes as Struts.
23. 1" ,, ,, ,, ,,
24. ¾" Sq. Steel Tubes as Struts (30 ton yield).
25. ⅞" ,, ,, ,, (30 ton yield).
26. 1" ,, ,, ,, (30 ton yield).
27. ¾" ,, ,, ,, (40 ton yield).
28. ⅞" ,, ,, ,, (40 ton yield).
29. 1" ,, ,, ,, (40 ton yield).
30. Moments of Inertia of Built-up Sections (Tables). } Connected.
31. Moments of Inertia of Built-up Sections (Instructions and Examples). }
32. Reinforced Concrete Slabs (Line Chart). } Connected.
33. Reinforced Concrete Slabs (Instructions and Examples) }
34. Capacity and Speed Chart for Troughed Band Conveyors.
35. Screw Propeller Design (Sheet 1, Diameter Chart). } Connected.
36. ,, ,, ,, (Sheet 2, Pitch Chart). }
37. ,, ,, ,, (Sheet 3, Notes and Examples) }
38. Open Coil Conical Springs.
39. Close Coil Conical Springs.
40. Trajectory Described by Belt Conveyors (Revised 1949).
41. Metric Equivalents.
42. Useful Conversion Factors.
43. Torsion of Non-Circular Shafts.
44. Railway Vehicles on Curves.
45. Chart of R.S. Angle Purlins.
46. Coned Plate Development.
47. Solution of Triangles (Sheet 1, Right Angles).
48. Solution of Triangles (Sheet 2, Oblique Angles).
49. Relation between Length, Linear Movement and Angular Movement of Lever (Diagram and Notes).
50. ,, ,, ,, ,, ,, ,, (Chart).
51. Helix Angle and Efficiency of Screws and Worms.
52. Approximate Radius of Gyration of Various Sections.

53. Helical Spring Graphs (Round Wire).
54. ,, ,, ,, (Round Wire).
55. ,, ,, ,, (Square Wire).
} Connected.

56. Relative Value of Welds to Rivets.
57. Ratio of Length/Depth of Girders for Stiffness.
58. Graphs for Strength of Rectangular Flat Plates of Uniform Thickness.
59. Graphs for Deflection of Rectangular Flat Plates of Uniform Thickness.
60. Moment of Resistance of Reinforced Concrete Beams.
61. Deflection of Leaf Spring.
62. Strength of Leaf Spring.
63. Chart Showing Relationship of Various Hardness Tests.
64. Shaft Horse Power and Proportions of Worm Gear.
65. Ring with Uniform Internal Load (Tangential Strain)
66. Ring with Uniform Internal Load (Tangential Stress)
} Connected.

67. Hub Pressed on to Steel Shaft. (Maximum Tangential Stress at Bore of Hub).
68. Hub Pressed on to Steel Shaft. (Radial Gripping Pressure between Hub and Shaft).
69. Rotating Disc (Steel) Tangential Strain.
70. ,, ,, ,, Stress.
} Connected.

71. Ring with Uniform External Load, Tangential Strain.
72. ,, ,, ,, ,, ,, Stress.
} Connected.

73. Viscosity Temperature Chart for Converting Commercial to Absolute Viscosities.
74. Journal Friction on Bearings.
75. Ring Oil Bearings.
76. Shearing and Bearing Values for High Tensile Structural Steel Shop Rivets, in accordance with B.S.S. No. 548/1934.
77. Permissible Compressive Stresses for High Tensile Structural Steel, manufactured in accordance with B.S.S. 548/1934.
} Connected.

78. Velocity of Flow in Pipes for a Given Delivery.
79. Delivery of Water in Pipes for a Given Head.
} Connected.

80. Working Loads in Mild Steel Pillar Shafts.
81. Involute Toothed Gearing Chart.
82. Steam Pipe Design. Chart Showing Flow of Steam Through Pipes.
83. Variation of Suction Lift and Temperature for Centrifugal Pumps.
84. Nomograph for Uniformly Distributed Loads on British Standard Beams.
85. ,, ,, ,, ,, ,,
86. ,, ,, ,, ,, ,,
87. Notes on Beam Design and on Use of Data Sheets, Nos. 84-5-6.
88. ,, ,, ,, ,, ,,
} Connected.

89. Curve Relating Natural Frequency and Deflection.
90. Vibration Transmissibility Curved or Elastic Suspension.
91. Instructions and Examples in the Use of Data Sheets, Nos. 89 and 90.
} Connected.

92. Pressure on Sides of Bunker.
93-4-5-6-7. Rolled Steel Sections.
98-99-100. Boiler Safety Valves.
101. Nomograph Chart for Working Stresses in Mild Steel Columns.
102. Presssure Required for Blanking and Piercing.
103. Punch and Die Clearances for Blanking and Piercing.
104. Nomograph for Valley Angles of Hoppers and Chutes.

(Data Sheets are 2d to Members, 4d to others, post free).

Orders for Pamphlets and Data Sheets to be sent to the Editor, *The Draughtsman*, cheques and orders being crossed "A.E.S.D."